Discovery of a Novel Class of Imidazo[1,2-a]Pyridines with Potent PDGFR Activity and Oral Bioavailability

Erik J. Hicken,* Fred P. Marmsater, Mark C. Munson, Stephen T. Schlachter, John E. Robinson, Shelley Allen, Laurence E. Burgess, Robert Kirk DeLisle, James P. Rizzi, George T. Topalov, Qian Zhao, Julie M. Hicks, Nicholas C. Kallan, Eugene Tarlton, Andrew Allen, Michele Callejo, April Cox, Sumeet Rana, Nathalie Klopfenstein, Richard Woessner, and Joseph P. Lyssikatos

Department of Drug Discovery, Array BioPharma, 3200 Walnut Street, Boulder, Colorado 80301, United States

S Supporting Information

ABSTRACT: The in silico construction of a PDGFRβ kinase homology model and ensuing medicinal chemistry guided by molecular modeling, led to the identification of potent, small molecule inhibitors of PDGFR. Subsequent exploration of structure−activity relationships (SAR) led to the incorporation of a constrained secondary amine to enhance selectivity. Further refinements led to the integration of a fluorine substituted piperidine, which resulted in significant reduction of P-glycoprotein (Pgp) mediated efflux and improved bioavailability. Compound **28** displayed oral exposure in rodents and had a pronounced effect in a pharmacokinetic−pharmacodynamic (PKPD) assay.

PDGFRβ cell IC$_{50}$ = 3 nM
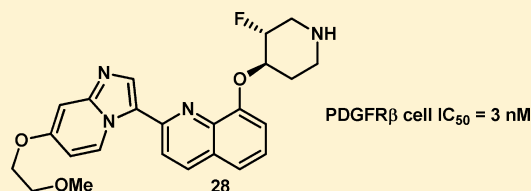
KEYWORDS: Platelet-derived growth factor, fluoro-piperidine, fluorine, Pgp

Platelet-derived growth factor receptor (PDGFR) is an attractive target for treating malignant disease.[1,2] Constitutive activation of PDGFR resulting from point mutations, chromosomal translocations, and autocrine loops have been described in gastrointestinal stromal tumors (GIST) and gliomas.[3] PDGFR also plays an important role in the remodeling and maintenance of blood vessels (neovasculature) through its regulation of pericytes, suggesting that inhibitors of PDGFR could have broad utility against a spectrum of human cancers as antiangiogenic agents.[4,5] In addition, PDGFR has been shown to be a potent mitogen for myofibroblast formation, a signature event in the progression of fibrosis.[6] The availability of a potent, selective, orally bioavailable PDGFR inhibitor would help define the role of the kinase in tumor growth, angiogenesis and fibrosis.

Although a few approved kinase inhibitors possess PDGFR inhibitory activity, their primary activity is targeted toward Abl or KDR, and dose escalation is often limited by attendant toxicities (i.e., Imatinib, Dasatinib, Sorafenib, Sunitinib, etc.). Prior to our investigation, two selective small-molecule inhibitors of PDGFR had been described in the literature.[7−9] We set out to discover and develop a novel, orally bioavailable, selective, and potent PDGFR antagonist using structure-based drug design strategies.

PDGFR belongs to the receptor tyrosine kinase class 3 (RTKIII), which comprises members of the PDGFR family, including PDGFRα, PDGFRβ, cKIT, cFMS, and FLT3. A highly related group of kinases include the VEGFR family, FLT1, FLT4, and KDR.[10−12] Although the sequence of PDGFR is known, there are no reported PDGFR crystal structures. The Protein Data Bank (www.pdb.org) does, however, include crystal structures of other members of the PDGFR and VEGFR families, namely, cFMS, cKIT, FLT3, KDR (VEGFR2), and FLT1 (VEGFR1). Many of these crystal structures also contain small molecule inhibitors cocrystallized in the ATP binding site. From this information, we can discern that there are minor protein sequence variations within the ATP binding pockets of these kinase families.[13] Our approach was to take advantage of the differences in sequence as well as the observed subtle differences in ATP-binding site shapes in order to impart the desired PDGFR selectivity to our inhibitors.

By using a published cFMS crystal structure and the known amino acid sequence of PDGFRβ, we constructed a model of PDGFRβ in silico. This model was then used to design novel small molecule antagonists containing an imidazopyridine to interact with the hinge region of PDGFRβ (Figure 1). Docking studies predicted that the addition of an amine would provide an interaction with the side chain of either an aspartic acid (i.e., ASP-111) or an asparagine (i.e., ASN-253) in the outer floor. The backbone carbonyl of arginine-252 was predicted to provide another polar interaction for a small molecule inhibitor. These interactions were predicted to provide compounds with good PDGFRβ potency, as well as potentially provide selectivity over members of the VEGFR family based on the expected variation in protein structure between kinases.[13] This effort culminated in the design of a novel series of imidazopyridines.[14]
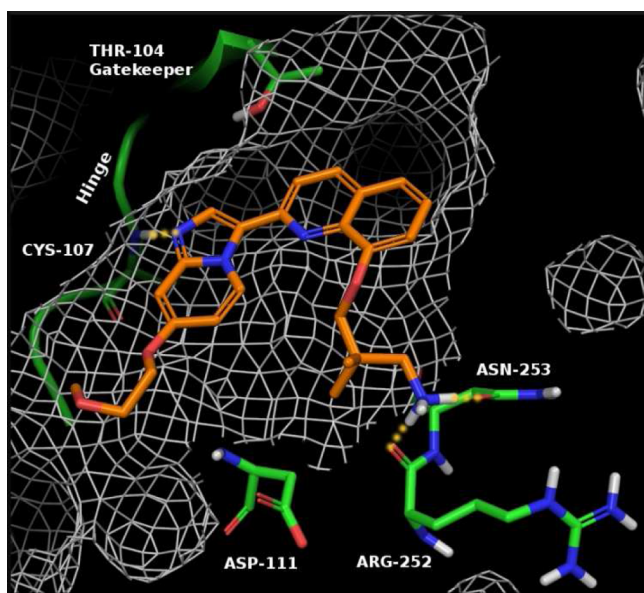
Figure 1. View of **1** docked into the ATP binding site of a PDGFRβ kinase homology model. Location of PDGFR residues are labeled for clarity.

An early example of this series (**1**, see Figures 1 and 2) demonstrated an IC$_{50}$ of 18 nM in our PDGFRβ cell assay.[15] A
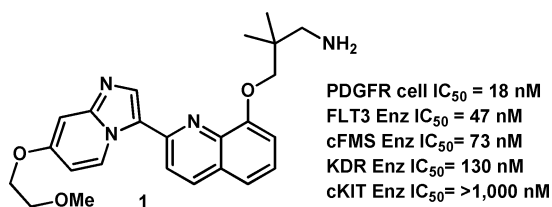

PDGFR cell IC$_{50}$ = 18 nM
FLT3 Enz IC$_{50}$ = 47 nM
cFMS Enz IC$_{50}$ = 73 nM
KDR Enz IC$_{50}$ = 130 nM
cKIT Enz IC$_{50}$ = >1,000 nM

Figure 2. Structure and activity profile for compound **1**.

molecular modeling view of compound **1** bound to the active site of PDGFRβ is shown in Figure 1, with the key residues highlighted. Although compound **1** was a potent PDGFRβ antagonist, selectivity over other members of the PDGFRβ and VEGFR families was limited (FLT3, cFMS, and KDR = <10×). We hypothesized that this poor selectivity was due to the high degree of conformational flexibility of the propyl-amine, allowing for a variety of polar interactions to be established within familial kinases. Consequently, we designed constrained analogues of **1** that could procure improved kinase selectivity (>10×) based on PDGFRβ specific residues.

With the identification of **1**, our medicinal chemistry efforts focused on the development of a synthetic route that would allow for late stage diversification of the amine headgroup. This effort resulted in a highly convergent synthesis that began with commercially available nitropyridine **2**, which was treated with 2-methoxyethanol in the presence of a strong base to provide chloropyridine **3**, which was used directly in the next step without purification. Compound **4** was obtained by the treatment of **3** with LiHMDS in the presence of Pd and X-Phos, followed by exposure to aqueous acid.[16] Cyclization of **4** was performed with aqueous chloroacetaldehyde at 50 °C to afford the key imidazopyridine **5**. The quinoline core was obtained by starting with commercially available quinoline diol **6**, which was exposed to benzyl bromide in the presence of K$_2$CO$_3$ to provide **7**. Treatment of quinolinol **7** with oxalyl

chloride and catalytic DMF in DCE at 85 °C provided the coupling partner **8** (Scheme 1).
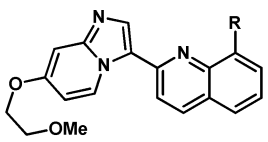
Scheme 1. Synthesis of Key Coupling Partners
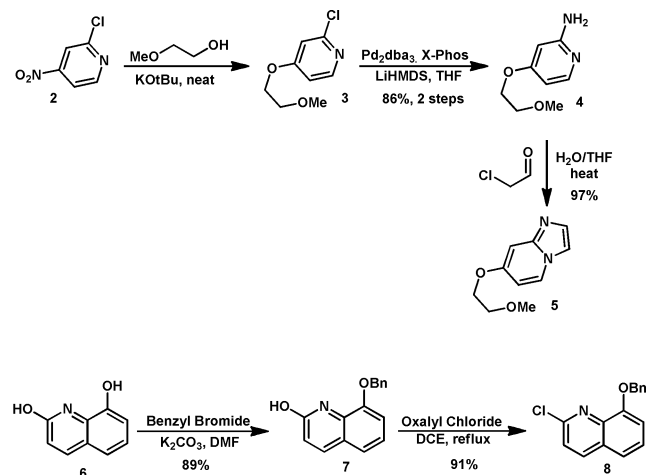
With the key partners in hand we were able to couple **5** and **8** via a Heck-type reaction using a mixed catalyst system of Pd(PPh$_3$)$_4$ and Pd(OAc)$_2$ in dioxane and water.[17,18] The residual benzyl protecting group was then removed using Pd(OH)$_2$ on carbon in the presence of ammonium formate to afford **9** (Scheme 2). This useful, advanced intermediate was
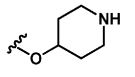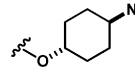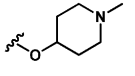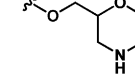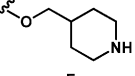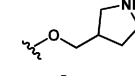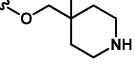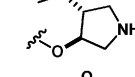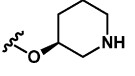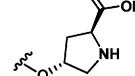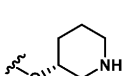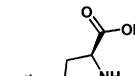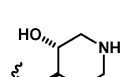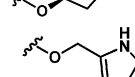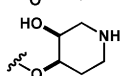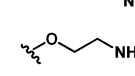
Scheme 2. Coupling and Alkylation Endgame of Synthesis
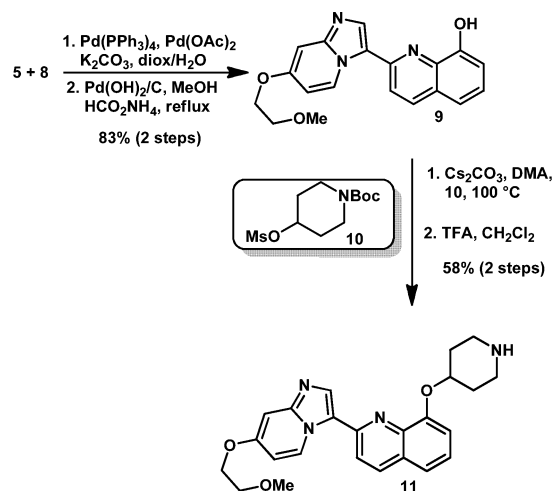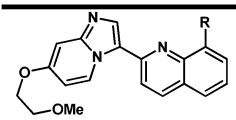
conveniently alkylated with mesylates such as **10** using Cs$_2$CO$_3$ in DMA to afford final products having an amine headgroup, after TFA-mediated removal of the BOC protecting group. This synthetic sequence was highly convergent and allowed for robust generation of diverse structure−activity relationships (SAR) around the amine headgroup, providing compounds such as **11**.
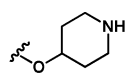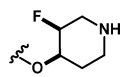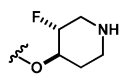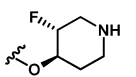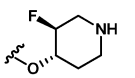
With the development of a robust synthesis for the formation of **9**, we began our refinement of **1** by searching for a constrained amine headgroup that would provide the desired selectivity (>10×) over members of the PDGFRβ and VEGFR families (Table 1). In general, the spatial orientation of the amine played an important role toward PDGFRβ potency and selectivity. With the aid of our PDGFRβ homology model, we found that it was possible to design an amine headgroup that

Table 1. In Vitro Potency of Compounds 11−26[a]

Compound	R	PDGFRβ Cell (nM)[b]	KDR Enz (nM)[c]	cFMs Enz (nM)[c]	Compound	R	PDGFRβ Cell (nM)[b]	KDR Enz (nM)[c]	cFMs Enz (nM)[c]
11	*(structure)*	3	39	>1,000	19‡	*(structure)*	28	203	>1,000
12	*(structure)*	9	42	312	20‡	*(structure)*	160	718	>1,000
13	*(structure)*	34	389	>1,000	21‡	*(structure)*	1	70	301
14	*(structure)*	1	51	88	22‡	*(structure)*	10	475	>1,000
15*	*(structure)*	5	102	21	23*	*(structure)*	958	77	>1,000
16*	*(structure)*	72	166	873	24*	*(structure)*	>1,000	173	>1,000
17‡	*(structure)*	3	ND	131	25	*(structure)*	>1,000	215	>1,000
18‡	*(structure)*	2	67	384	26	*(structure)*	176	206	>1,000

[a]Key: ‡, denotes racemic compound, relative stereochemistry is as depicted; *, denotes single enantiomer. ND = not determined. [b]All compounds with PDGFR IC$_{50}$ values of <100 nM were run at least in duplicate. [c]All compounds were run in this assay at least in duplicate; value shown is an average of the assay results.

Table 2. In Vitro Profile of Compounds 11 and 27−29[a]

	11	cis-27	trans-27	28‡	29‡
(core structure)	*(structure)*	*(structure)*	*(structure)*	*(structure)*	*(structure)*
PDGFRβ cell IC$_{50}$ (nM)	3	4	4	3	3
PDGFRβ cell + 50% HP IC$_{50}$ (nM)	25	25	63	70	55
Flt3 Enz IC$_{50}$ (nM)	2	4	3	10	8
KDR Enz IC$_{50}$ (nM)	39	28	20	53	16
cKit Enz IC$_{50}$ (nM)	961	>1,000	682	430	491
cFMS Enz IC$_{50}$ (nM)	>1,000	282	767	322	499
CYP p450 (nM) (1A2, 2C19, 2C9, 2D6, 3A4)	>10,000	>10,000*	>10,000	>10,000	>10,000
Microsomal Clearance (%ER) (Mouse, Rat, Cyno, Human)	63, 26, 85, 28	70, 33, 78, 33	58, 30, 87, 53	54, 34, 88, 58	57, 34, 89, 58
Parental LLC/PK1 (Papp AB, 1x10^{-6} cm/s)	16.3 ± 0.9	2.7 ± 0.1	4.4 ± 0.3	3.7 ± 0.4	---
MDR1 LLC/PK1 (Pe Ratio, AB/BA)	5.7	1.8	1.1	1.4	---
Measured pKa	9.3	7.5	7.4	---	---

[a]Key: *, compound cis-27 had an IC$_{50}$ of 5880 nM on CYP 2D6; ‡, the absolute stereochemistry of 28 and 29 are arbitrarily assigned.

would provide good PDGFRβ potency and improved kinase selectivity when compared to **1**. Surprisingly, some amine headgroups were found to provide analogues having excellent selectivity over cFMS and cKIT (>100×), despite the same amino acid residues being located at the outer floor of the binding pocket. This is potentially due to the specific location of the polar residues in the outer floor of PDGFRβ, such as ASP-111 and ARG-252, and our use of a rigid amine headgroup. In addition, we found that >10× selectivity[15] over KDR could be obtained with a variety of amine headgroups (**14**, **15**, **18**, **21**, and **22**), with the observed increase in PDGFRβ potency likely due to optimized binding with the polar residues in the outer floor. Some flexibility in the distance between the quinolone and amine NH was tolerated, with 2 to 3 carbon atoms between the quinoline oxygen and amine appearing optimal in cyclized amines (i.e., **11** and **15**) but an optimal length was observed (**11** vs **19**). Secondary cyclic amines were preferred over primary acyclic amines (**1** and **26** vs **11**). It was found that pyrrolidine headgroups were well tolerated (**21** and **22**) except when the carbon adjacent to the amine was substituted (**23** and **24**). Alkylation of the amine (**12**) decreased PDGFRβ potency while leaving KDR potency unchanged. In addition, it was determined that the absolute configuration of a chiral amine can play a significant role in potency (**15** vs **16**).

After substantial effort we determined that compound **11** had achieved the target properties of potency and selectivity (>10× over KDR and >100× over cFMS, see Table 1) providing the desired improvements over **1**.[15] Although we had discovered alternative compounds that were more potent than **11**, the overall in vitro properties of **11** were superior. This determination was based on a combination of properties, including stability (i.e., **14** had >70% microsomal clearance in rodents and cyno), low cell shift in the presence of human plasma (i.e., PDGFRβ cellular assay run in the presence of 50% human plasma; **21** = 29 nM, **22** = >1000 nM), and selectivity over members of the RTKIII family.[15] The profile of **11** is summarized in Table 2. Our lead compound **11** had excellent selectivity over cKIT and cFMS (>100×), was clean on all tested subtypes of cytochrome p450 (>10 μM), and was potent in the cellular assay in the presence of 50% human plasma (25 nM). Subsequently, **11** was progressed to rat PK, which revealed that compound **11** suffered from poor oral exposure (16% F, dosed as a 20% Solutol aqueous solution, see Table 3).

Table 3. Male Rat PK Profile of Compounds 11, 27, and 28

male rat PK		**11**	*cis*-**27**	*trans*-**27**	**28**
1 mg/kg IV	CL (mL/min/kg)	33	28	24	20
	ER	48	41	34	29
10 mg/kg PO	AUC (μg)(hr)/mL	0.80	0.73	2.1	2.3
	C_{max} (μg/mL)	0.07	0.07	0.12	0.16
	% F	16	13	30	28

These data, in combination with moderate IV clearance and excellent solubility (>1000 μg/mL) suggested that the poor oral exposure was not solely due to in vivo instability. Compound **11** was analyzed in a MDR1 cell line assay, and although attenuated apical recoveries were noted (50% recovery), it displayed high passive permeability along with efflux transport by P-glycoprotein (Pgp) (Pe ratio = 5.7).

The measured pK_a of **11** was found to be 9.3, which facilitated good solubility but potentially played a role in Pgp

efflux. By attenuating the pK_a of the piperdine amine, we hoped to positively influence passive permeability[19−22] and reduce Pgp mediated efflux.[23−25] Attempts had been made earlier to reduce the pK_a of **11** by employing a morpholine headgroup (**20**), installing an ether or hydroxyl on the ring (**17**, **18**, and **22**), moving the amine closer to the ether linkage (**15** and **26**) or installing an ester adjacent to the amine (**23** and **24**). Unfortunately, these attempts either decreased PDGFRβ potency or led to high predicted microsomal clearance.

Our focus then turned to the utility of fluorine. It is well precedented that introduction of a highly polarized and strong C−F bond (105 kcal/mol) can reduce the basicity of proximal amines.[26,27] In addition, installation of fluorine not only creates a strong C−F bond but also leads to increases in the strength of adjacent C−O and C−C bonds.[28,29] Therefore, the addition of fluorine on the piperidine ring had the potential to not only attenuate the amine basicity but also enhance metabolic stability.

Accordingly, we installed a single fluorine atom on the piperidine ring (Table 2), arriving at two racemic but diastereomerically pure compounds, *cis*-**27** and *trans*-**27**. For cyclic alkyl amines, the decrease of pK_a from an axial fluorine substituent can be considerably smaller than that seen for an equatorial fluorine.[23−25] Therefore, the relative orientation of the fluorine substituent can have an effect on the pK_a of the piperidine amine. On the basis of our experimental measurement, we found that the fluorine atom had attenuated the pK_a nearly two units, from 9.3 for compound **11** to 7.4 for *trans*-**27**. Although we had anticipated a difference in the pK_a of *cis*-**27** and *trans*-**27**, they were essentially the same.

We anticipated that the observed decrease in pK_a of the piperidine amine would be sufficient to increase the passive permeability of **11** while decreasing Pgp mediated efflux and lead to improved bioavailability.[19−25] During our in vitro profiling of these compounds, we were surprised to find that installation of a fluorine atom on the piperidine ring had caused a *reduction* in the apparent permeability of both *cis*- and *trans*-**27** when compared to compound **11** (albeit with attenuated apical recoveries of 30% for **27**). This result is in contrast to our previous experience, as well as literature precedents that suggest a more neutral species (i.e., decreasing the pK_a of a basic amine) will improve membrane permeability.[19−25] Although the apparent permeability of *cis*-**27** and *trans*-**27** had been reduced, Pgp mediated efflux was significantly decreased, as seen in the MDR1 cell line assay, when compared to **11**.

Both *cis*- and *trans*-**27** were then progressed into rat pharmacokinetic studies. The results demonstrate that the installation of fluorine clearly reduced the IV clearance, from 33 (**11**) to 24 mL/min/kg (*trans*-**27**). Despite the improvement in IV clearance, *cis*-**27** was unexpectedly indistinguishable from **11** in rat PK (Table 3). Conversely, *trans*-**27** had significantly better in vivo exposure (2−3× improved AUC, C_{max}, and % F) than *cis*-**27** and **11**. We were gratified to find that the installation of a single fluorine atom had not only aided in maintaining the desired potency and selectivity but provided a significant improvement in oral bioavailability.

With the identification of *trans*-**27**, we separated and profiled the enantiomers **28** and **29**, to determine if they would differentiate (the absolute stereochemistry shown for **28** and **29** are arbitrarily assigned). These two compounds were nearly identical in all assays with the exception of the KDR enzyme assay, in which **28** was 53 nM on KDR and 17× selective for PDGFRβ, versus the less selective **29**, which was 16 nM on

81

dx.doi.org/10.1021/ml4003953 | *ACS Med. Chem. Lett.* 2014, 5, 78−83

KDR and only 5× selective for PDGFRβ.[15] When fluoro piperdine **28** was evaluated in vitro, it was found to maintain the desirable properties of **11** while improving upon **11** by lowering Pgp efflux. Oral exposure of **28** in rat was improved when compared to **11** with a concomitant decrease in IV clearance (see Table 3).

Compound **28** was also evaluated in a pharmacokinetic−pharmacodynamic (PKPD) assay, which we employed as a surrogate for the efficacy of our PDGFR inhibitors (Figure 3).
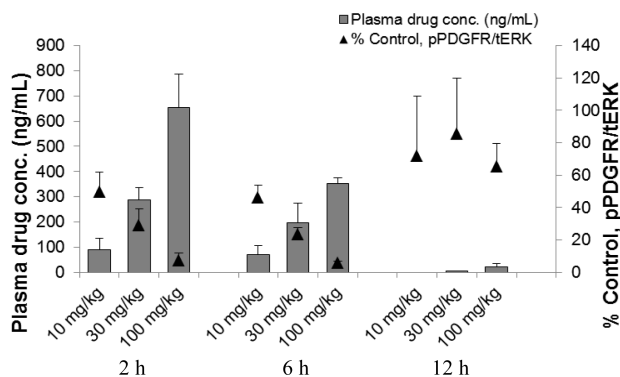

Figure 3. PKPD study of compound **28** as a single oral dose. Multiple time points and doses were evaluated. The ratio of pPDGFR/tERK was measured and compared to control.

The PKPD experiment was performed in female nude mice bearing subcutaneous C6 tumor xenografts. pPDGFR levels were determined and the values normalized to TotalERK by Western Blot. Compound **28** was evaluated at three different time points and at three doses. Following oral administration of **28** as a single dose, a PD response was observed in a dose-dependent manner. The effect of **28** was maximized at the 6 h time point with pPDGFR levels returning to those of the control after 12 h. On the basis of this data, the EC$_{50}$ of **28** was determined to be a total drug concentration of 65 ng/mL.

Compound **28** was determined to be an excellent compound for the investigation of PDGFRβ inhibition in rodents and was well tolerated on chronic PO dosing in rats at doses of up to 50 mg/kg BID for two weeks. However, it suffered from high clearance in cynomolgus monkeys (see Table 4), which was predicted by the in vitro microsome stability assay of **28** (Table 2). The resulting lack of exposure in monkeys prevented tolerability assessment in second species and prohibited additional studies. Within this series we have established robust IV/IV correlation in both rat and monkeys. As these analogues consistently display high first pass clearance in second species, complicating preclinical toxicology assessment, we continued our medicinal chemistry efforts toward the development of a compound with improved oral exposure and decreased clearance in second species. These efforts will be addressed in a subsequent manuscript.

■ ASSOCIATED CONTENT

ⓢ Supporting Information
Protocol of the PDGFR cellular assay and pharmacokinetic/pharmacodynamic assay. Experimental procedures for the synthesis and chacterization of **3**−**11**, **27**, and **28**. This material is available free of charge via the Internet at http://pubs.acs.org.

■ AUTHOR INFORMATION

Corresponding Author
*(E.J.H.) Tel: 303-386-1282. E-mail: erik.hicken@arraybiopharma.com.

Notes
The authors declare no competing financial interest.

■ ACKNOWLEDGMENTS

■ ABBREVIATIONS

AUC, total area under the plasma drug concentration−time curve; DBA(dba), dibenzylideneacetone; DCE, 1,1-dichloroethane; ER, extraction ratio; HMDS, 1,1,1,3,3,3-hexamethyldisilazane; MDR1, multidrug resistance gene; PDGFR, platelet-derived growth factor receptor; Pgp, P-glycoprotein; PK, pharmacokinetic; pK_a, logarithmic acid dissociation constant; PKPD, pharmacokinetic−pharmacodynamic; SAR, structure−activity relationship; TFA, trifluoroacetic acid; X-Phos, 2-dicyclohexylphosphino-2′,4′,6′-triisopropylbiphenyl

■ REFERENCES

(1) Lewis, N. L. The platelet-derived growth factor receptor as a therapeutic target. *Curr. Oncol. Rep.* **2007**, *9*, 89−95.

(2) Board, R.; Jayson, G. C. Platelet-derived growth factor receptor (PDGFR): A target for anticancer therapeutics. *Drug Resist. Updates* **2005**, *8*, 75−83.

(3) Wong, N. A. C. S.; Mangwana, S. KIT and PDGFRα mutational analyses of mixed cell-type gastrointestinal stromal tumors. *Histopathology* **2007**, *51*, 758−762.

(4) Joyce, J. A. Therapeutic targeting of the tumor microenvironment. *Cancer Cell* **2005**, *7*, 513−520.

(5) Huang, J.; Soffer, S. Z.; Kim, E. S.; McCrudden, K. W.; Huang, J.; New, T.; Manley, C. A.; Middlesworth, W.; O'Toole, K.; Yamashiro, D. J.; Kandel, J. Vascular remodeling marks tumors that recur during chronic suppressionof angiogenesis. *J. Mol. Cancer Res.* **2004**, *2*, 36−42.

(6) Bonner, J. C.; Lindroos, P. M.; Rice, A. B.; Moomaw, C. R.; Morgan, D. L. Induction of PDGF receptor-α in rat myofibroblasts during pulmonary fibrogenesis in vivo. *Am. J. Physiol.: Lung Cell. Mol. Physiol.* **1998**, *274*, L72−L80.

(7) Matsuno, K.; Nakajima, T.; Ichimura, M.; Giese, N. A.; Yu, J.-C.; Lokker, N. A.; Ushiki, J.; Ide, S.; Oda, S.; Nomoto, Y. Potent and selective inhibitors of PDGFR receptor phosphorylation. 2. Synthesis, structure activity relationship, improvement of aqueous solubility, and biological effects of 4-[4-(*N*-substituted(thio)carbamoyl)-1-piperazin-

Table 4. hERG and Cyno PK Profile of 28

PDGFRβ Cell IC$_{50}$ (nM)		3
hERG IC$_{50}$		3.9 μM
	AUC (μg)(hr)/mL	0.95
Cyno PK	CMax (μg/mL)	0.19
30 mg/kg PO	ER	71
	%F	6

yl]-6,7-dimethoxyquinazoline derivatives. *J. Med. Chem.* **2002**, *45*, 4513−4523.

(8) Roberts, W. G.; Whalen, P. M.; Soderstrom, E.; Moraski, G.; Lyssikatos, J. P.; Wang, H.-F.; Cooper, B.; Baker, D. A.; Savage, D.; Dalvie, D.; Atherton, J. A.; Ralston, S.; Szewc, R.; Kath, J. C.; Lin, J.; Soderstrom, C.; Tkalcevic, G.; Cohen, B. D.; Pollack, V.; Barth, W.; Hungerford, W.; Ung, E. Antiangiogenic and antitumor activity of a selective PDGFR tyrosine kinase inhibitor, CP-673,451. *Cancer Res.* **2005**, *65*, 957−966.

(9) For a more recent review see: Dai, Y. Platelet-derived growth factor receptor kinase inhibitors: a review of the recent patent literature. *Expert Opin. Ther. Patents* **2010**, *20*, 885−907.

(10) Robinson, D. R.; Wu, Y.-M.; Lin, S.-F. The protein tyrosine kinase family of the human genome. *Oncogene* **2000**, *19*, 5548−557.

(11) Ullrich, A.; Schlessinger, J. Signal transduction by receptors with tyrosine activity. *Cell* **1990**, *61*, 203−212.

(12) Kaipainen, A.; Korhonen, J.; Pajusola, K.; Aprelikova, O.; Persico, M. G.; Terman, B. I.; Alitalo, K. The related FLT4, FLT1, and KDR receptor tyrosine kinases show distinct expression patterns in human endothelial cells. *J. Exp. Med.* **1993**, *178*, 2077−2088.

(13) Please see the Supporting Information to view key protein sequence variations that are within the active site.

(14) Allen, S.; Greschuk, J. M.; Kallan, N. C.; Marmsater, F. P.; Munson, M. C.; Rizzi, J. P.; Robinson, J. E.; Schlachter, S. P.; Topalov, G. T.; Zhao, Q. Imidazo[1,2-A] Pyridine Compounds as Receptor Tyrosine Kinase Inhibitors. International Patent Application WO 2008/124323 A1, 2008.

(15) We experienced difficulties obtaining a reproducible PDGFR enzyme assay and chose to use a more robust cellular assay for the screening of our compounds.

(16) Huang, X.; Buchwald, S. L. New ammonia equivalents for the Pd-catalyzed amination of aryl halides. *Org. Lett.* **2001**, *3*, 3417−3419.

(17) Touré, B. B.; Lane, B. S.; Sames, D. Catalytic C−H arylation of SEM-protected azoles with palladium complexes of NHCs and phosphines. *Org. Lett.* **2006**, *8*, 1979−1982.

(18) Koubachi, J.; El Kazzouli, S.; Berteina-Raboin, S.; Mouaddib, A.; Guillaumet, G. Regioselective palladium-catalyzed arylation and heteroarylation of imidazo[1,2-a]pyridines. *Synlett* **2006**, *19*, 3237−3242.

(19) Faller, B.; Urban, L.; Mannhold, R. *Hit and Lead Profiling: Identification and Optimization of Drug-Like Molecules*; Wiley-VCH: Berlin, Germany, 2009.

(20) Kerns, E. H.; Di, L. *Drug-Like Properties: Concepts, Structure Design and Methods: from ADME to Toxicity Optimization*; Academic Press: New York, 2008.

(21) Gleeson, M. P. Generation of a set of simple, interpretable ADMET rules of thumb. *J. Med. Chem.* **2008**, *51*, 817−834.

(22) Thomas, V. H.; Bhattachar, S.; Hitchingham, L.; Zocharski, P.; Naath, M.; Surendran, N.; Stoner, C. L.; El-Kattan, A. The road map to oral bioavailability: an industrial perspective. *Expert Opin. Drug Metab. Toxicol.* **2006**, *2*, 591−608.

(23) Lerchner, A.; Machauer, R.; Betschart, C.; Veenstra, S.; Rueeger, H.; McCarthy, C.; Tintelnot-Blomley, M.; Jaton, A.-L.; Rabe, S.; Desrayaud, S.; Enz, A.; Staufenbiel, M.; Paganetti, P.; Rondeau, J.-M.; Neumann, U. Macrocyclic BACE-1 inhibitors acutely reduce Aβ in brain after po application. *Bioorg. Med. Chem. Lett.* **2010**, *20*, 603−607.

(24) Su, D.-S.; Lim, J. L.; Tinney, E.; Wan, B.-L.; Murphy, K. L.; Reiss, D. R.; Harrell, C. M.; O'Malley, S. S.; Ransom, R. W.; Chang, R. S. L.; Pettibone, D. J.; Yu, J.; Tang, C.; Prueksaritanont, T.; Freidinger, R. M.; Bock, M. G.; Anthony, N. J. 2-Aminobenzophenones as a novel class of bradykinin B1 receptor antagonists. *J. Med. Chem.* **2008**, *51*, 3946−3952.

(25) Cox, C. D.; Breslin, M. J.; Whitman, D. B.; Coleman, P. J.; Garbaccio, R. M.; Fraley, M. E.; Zrada, M. M.; Buser, C. A.; Walsh, E. S.; Hamilton, K.; Lobell, R. B.; Tao, W.; Abrams, M. T.; South, V. J.; Huber, H. E.; Kohl, N. E.; Hartman, G. D. Kinesin spindle protein (KSP) inhibitors. Part V: Discovery of 2-propylamino-2,4-diaryl-2,5-dihydropyrroles as potent, water-soluable KSP inhibitors, and modulation of their basicity by b-fluorination to overcome cellular

efflux by P-glycoprotein. *Bioorg. Med. Chem. Lett.* **2007**, *17*, 2697−2702.

(26) Morgenthaler, M.; Schweizer, E.; Hoffmann-Roder, A.; Benini, F.; Martin, R. E.; Jaeschke, G.; Wagner, B.; Fischer, H.; Bendels, S.; Zimmerli, D.; Schneider, J.; Diederich, F.; Kansy, M.; Muller, K. Predicting and tuning physicochemical properties in lead optimization: Amine basicities. *ChemMedChem* **2007**, *2*, 1100−1115.

(27) van Niel, M. B.; Collins, I.; Beer, M. S.; Broughton, H. B.; Cheng, S. K. F.; Goodacre, S. C.; Heald, A.; Locker, K. L.; MacLeod, A. M.; Morrison, D.; Moyes, C. R.; O'Connor, D.; Pike, A.; Rowley, M.; Russel, M. G. N.; Sohal, B.; Stanton, J. A.; Thomas, S.; Verrier, H.; Watt, A. P.; Castro, J. L. Fluorination of 3-(3-(piperdin-1-yl)propyl)-indoles and 3-(3-(piperazin-1-yl)propyl)indoles gives selective human 5-HT$_{1D}$ receptor ligands with improved pharmacokinetic profiles. *J. Med. Chem.* **1999**, *42*, 2087−2104.

(28) Meanwell, N. A. Synopsis of some recent tactical application of bioisosteres in drug design. *J. Med. Chem.* **2011**, *54*, 2529−2591.

(29) Purser, S.; Moore, P. R.; Swallow, S.; Gouverneur, V. Fluorine in medicinal chemistry. *Chem. Soc. Rev.* **2008**, *37*, 320−330.